Editors' Suggestion

Positron-Induced Luminescence

E. V. Stenson,[1,*] U. Hergenhahn,[1,2] M. R. Stoneking,[1,3] and T. Sunn Pedersen[1,4]
[1]Max Planck Institute for Plasma Physics, 17491 Greifswald and 85748 Garching, Germany
[2]Leibniz Institute of Surface Engineering (IOM), 04318 Leipzig, Germany
[3]Department of Physics, Lawrence University, Appleton, Wisconsin 54911, USA
[4]University of Greifswald, 17489 Greifswald, Germany

(Received 25 September 2017; published 5 April 2018)

We report on the observation that low-energy positrons incident on a phosphor screen produce significantly more luminescence than electrons do. For two different wide-band-gap semiconductor phosphors (ZnS:Ag and ZnO:Zn), we compare the luminescent response to a positron beam with the response to an electron beam. For both phosphors, the positron response is significantly brighter than the electron response, by a factor that depends strongly on incident energy (0–5 keV). Positrons with just a few tens of electron-volts of energy (for ZnS:Ag) or less (for ZnO:Zn) produce as much luminescence as is produced by electrons with several kilo-electron-volts. We attribute this effect to valence band holes and excited electrons produced by positron annihilation and subsequent Auger processes. These results demonstrate a valuable approach for addressing long-standing questions about luminescent materials.

DOI: 10.1103/PhysRevLett.120.147401

Cathodoluminescent materials, in addition to being widespread in consumer devices, are important scientific tools for diagnosing charged particle beams, short-wavelength photons, and non-neutral plasmas. Despite decades of use, however, some important aspects of the physics of phosphors remain topics of debate and investigation [1–3]. Depending on the material, this may include the structure of luminescence centers [3,4], the excitation and relaxation pathways [1,5], and/or the origin of the dead voltage [2,6]. (For most phosphors, no luminescence is observed when incident electrons' kinetic energy is below some threshold, which is usually orders of magnitude larger than the material's band gap. The transition to the linear regime, in which an increase in electron beam energy produces a proportional increase in the number of photons produced, may not occur until the energy exceeds several kilo-electron-volts.) Yet another question involving phosphors is a practical one; although they are routinely used for diagnosing both matter and antimatter systems [7], comparisons between the two seem to be scarce. Quantitative studies of positron luminescence with higher-energy beams ($\geq$ 30 keV) have been performed on two materials [anthracene and (ZnS, CdS):Ag], in which no significant differences from the electron response were observed [8,9]; a qualitative study at lower energies found spectral differences in luminescence from 3-keV positrons versus 2-keV electrons incident on an anthracene-polystyrene solution [10]. However, we were unable to find in the electronically searchable literature a quantitative comparison of the luminescence produced by low-energy (0–5 keV) positrons and electrons incident on a phosphor, despite this being highly relevant for diagnosing non-neutral plasmas and positron beams used in surface science.

In this Letter, for two different phosphors (ZnS:Ag and ZnO:Zn, which have notably large and notably small dead voltages, respectively), we quantitatively compare the luminescence excited by a positron beam to that excited by an electron beam with a comparable particle flux, for incident energies ranging from 0 to 5 keV. In this regime, penetration depths into solid matter range from less than a single atomic layer [11] up to a few hundred nanometers [12], and surface studies with positrons have produced a wealth of new findings through a variety of methods [13–15]. Our results put the widespread use of phosphors for diagnosis in antimatter physics on a sounder footing, while at the same time offering insights into the properties of phosphors and the mechanisms of cathodoluminescence.

The luminescent efficiency of electron beams has been studied for a number of materials and beam properties [6,16–18]. Luminescence can be expressed as the product of independent functions of the electron beam energy and beam current, with a linear dependence on current up to current densities far higher than pertains to our work [6,19]. We assert that positron response can be described by an expression of the same form and therefore write

$$L_{\pm} = g_{1\pm}(I) g_{2\pm}(V) \tag{1}$$

$$= I g_{\pm}(V), \tag{2}$$

where the subscript + (−) refers to positrons (electrons), L is luminescence, and g_1 and g_2 are independent functions of the unsigned, single-species beam current I and the attractive phosphor screen bias V, respectively. (For electrons, $V = V_{\text{screen}}$, while for positrons, $V = -V_{\text{screen}}$.) In

Eq. (2), we have used $g_1(I) = kI$, and the constant k has been incorporated into g. Naively, one would also expect dg/dV to be constant as soon as eV (where e is the elementary charge) exceeds the band gap of the material (e.g., 3.5 or 3.9 eV for ZnS, depending on the polymorph; 3.3 eV for ZnO). For electrons at energies of 10–30 keV (typical of cathode ray tubes), this is indeed the case; an increase in V results in a proportional increase in the number of electron-hole pairs, which in turn generate photons at luminescence centers. At lower voltages, however, it is not; 1–2 kV may need to be applied to produce any detectable luminescence at all, and the transition to linearity may require several more kilovolts. The value of the "dead voltage," the V intercept of the linear part of $g_-(V)$, varies with the type of phosphor and its preparation [6]. Electron data exhibiting typical screen-bias dependence are shown in Fig. 1. The corresponding positron data plotted alongside illustrate that not only is positron luminescence brighter than electron luminescence, but it also has a distinct functional dependence on incident particle energy.

Experiments were conducted with two different phosphor screens. The first was commercially produced (Kimball Physics) and uses ZnS:Ag type 1330 (P-22 Blue).

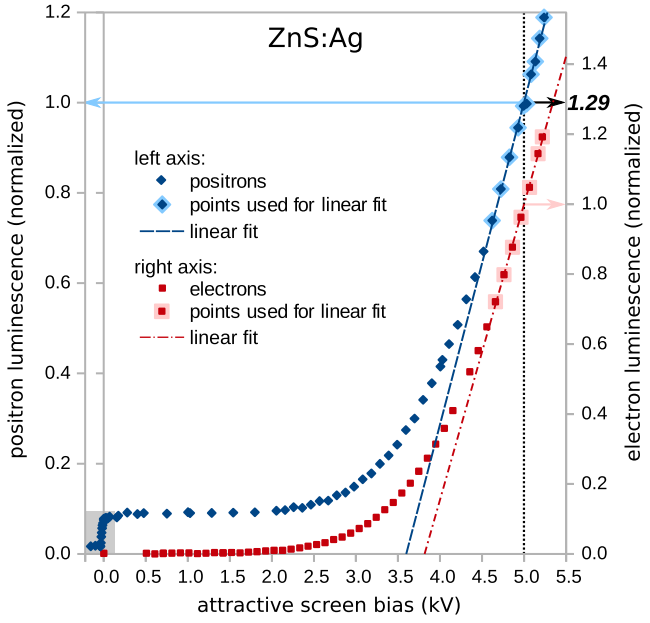

FIG. 1. Dependence of ZnS:Ag luminescence on attractive screen bias for positrons (blue diamonds, left y axis) and electrons (red squares, right y axis). Each data set is independently normalized to the 5 kV value; uncertainties are on the order of the symbol size or smaller. To facilitate comparisons of absolute luminescence at a glance, the relative scaling of the two vertical axes is chosen to match measurements of luminescence yield; this interspecies comparison, however, has a larger uncertainty. For example, at $V = 5$ kV, positrons produce $L_+/L_- = 1.29 \pm 0.08$ as much luminescence as electrons. The gray box indicates the region shown in greater detail in Fig. 5.

The phosphor layer, applied to a conductive glass plate in a stainless steel holder, is 50–70 μm thick, corresponding to 10–20 layers of ~5-μm phosphor particles. The second screen uses an identical plate and holder, to which we applied the phosphor ZnO:Zn (Leuchtstoff GmbH Heidelberg), which is known for its responsiveness to low-energy electrons (implying an unusually low dead voltage), via an ethanol suspension and a standard-issue paintbrush. Neither screen had an aluminum layer or a bonding agent (two frequent additions to phosphor screens), so that incident charged particles would interact directly with the phosphor. Each screen could be biased positively or negatively to about 5 kV. Luminescence produced by charged particles was measured by photographing the phosphor layer through the glass plate with a cooled CCD camera (Apogee), subtracting a background image, and then summing the pixel counts over a region larger than the beam size. Exposure lengths ranged from 30 to 300 s. Example data can be found in the Supplemental Material [20].

The positron beam system (First Point Scientific) uses positrons from a ^{22}Na source (2–4 mCi) that are moderated in a thick layer of solid neon; the beam current was < 0.15 pA. In order to produce an electron beam for comparison with the positron beam, the moderator was negatively biased to repel secondary electrons produced by the moderation process; the resulting electron beam was then attenuated with a more negative retarding potential to produce beam currents of 0.02–2 pA. Each beam was adiabatically magnetically guided ($B = 120$–800 G) around a line-of-sight shield (filtering away unmoderated positrons), then through two sets of cylindrical electrodes en route to the phosphor screen in ultrahigh vacuum (10^{-10} mbar). Select electrodes could be used to attenuate the beam or to measure the beams' longitudinal energy distributions (Fig. 2); all others were grounded. A typical energy distribution measurement for each species can be found in the Supplemental Material [20]. The parallel temperature is on the order of a few electron-volts (2 eV for

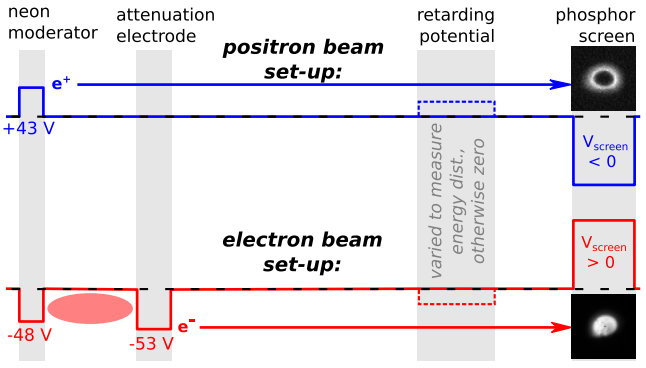

FIG. 2. Illustration of typical electrostatic bias voltages used for positron (top) and electron (bottom) experiments, plus an example image of each beam.

the electron beam, 6 eV for the positron beam); the perpendicular temperature is expected to be of the same order or less. Thus, the energy spread is small compared to the particles' incident energy for typical (kilovolt-scale) values of V.

As expressed in Eqs. (1) and (2), precise measurements of I are needed to make absolute comparisons between positron and electron luminescence; for the ∼0.1-pA positron beam, the current had to be determined to an accuracy of a few thousandths of a picoampere. These were performed with the screen connected to ground through a picoammeter (Keithley). Corresponding luminescence measurements for each beam current were taken at an attractive screen bias of several kilovolts. In all four cases (for both species and both phosphors), this yielded as expected a linear relationship betwen L and I [Eq. (2)]; additional details and plots can be found in the Supplemental Material [20]. The assumption that L depends on V and I independently was also observed experimentally. For a given species and phosphor, so long as $eV \gg$ the beam energy, varying the phosphor screen bias always produces the same $g(V) = L(V)/I$ curve. This curve is different, however, for each pairing of species and phosphor. Both species' curves are plotted in Fig. 1 for ZnS:Ag and in Fig. 3 for ZnO:Zn.

For ZnS:Ag (Fig. 1), the electron curve $g_-(V)$ exhibits the standard nonresponsiveness at low voltages and transitions to linear behavior for $V \geq 4.6$ kV. A fit to points in the linear regime yields a dead voltage of 3.82 ± 0.02 kV for a 50-eV beam. The positron curve $g_+(V)$ also exhibits linear dependence for $V \geq 4.6$ kV but has a somewhat lower dead voltage (3.60 ± 0.02 kV for a 45-eV beam). Most strikingly, $g_+(V)$ does not go to zero as $V \to 0^+$ but rather plateaus. The phosphor screen responds to positrons at attractive screen biases well below the threshold for significant electron response, persists even for a positively biased screen, and only disappears when the screen is biased repulsively to within about 10 eV of the beam energy. The small remaining luminescence beyond the cutoff ($V < -40$ V) constitutes a little less than 2% of the total luminescence at $V = 5$ keV and can be attributed to a small population of high-energy positrons (> 150 eV) also seen in the beam energy distribution measurement [20].

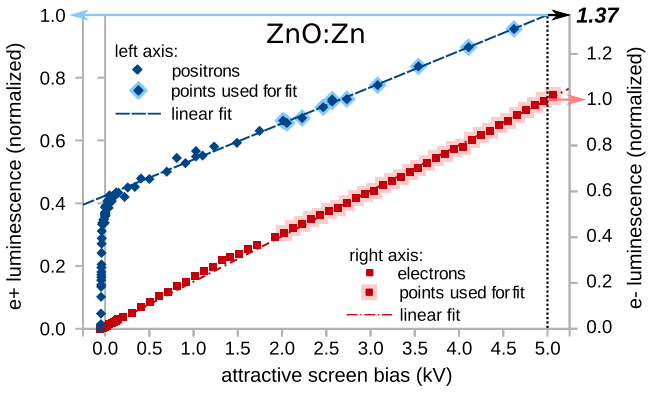

FIG. 3. Dependence of ZnO:Zn luminescence on attractive screen bias is plotted for positrons and electrons in the same fashion as in Fig. 1. The relative luminescence yield L_+/L_- at $V = 5$ kV is 1.37 ± 0.15.

For ZnO:Zn (Fig. 3), no dead voltage is identifiable for either species; both positrons and electrons produce luminescence as soon as they have enough kinetic energy to reach the screen—i.e., the V threshold for detection of luminescence from a repulsively biased screen is located precisely at the beam energy. The $g_-(V)$ and $g_+(V)$ curves are nevertheless highly distinct for this phosphor as well. Whereas $g_-(V)$ is almost perfectly linear over the entire range of our measurements, $g_+(V)$ initially rises orders of magnitude faster, with the same width in V as the beam's energy distribution measurement. In other words, as soon as positrons can reach the screen electrostatically, they produce as much luminescence as electrons with ∼2.5 keV of kinetic energy.

Comparisons such as this (of the absolute luminescence of one species to the other) follow from the current calibration—i.e., how many image counts are generated per picoampere of positrons or electrons. Results indicate that for the same I, 5-keV positrons produce more luminescence than 5-keV electrons by a factor of $(L_+/L_-)|_{5\text{ kV}} = g_+(5\text{ kV})/g_-(5\text{ kV}) = 1.29 \pm 0.08$ for ZnS:Ag and 1.37 ± 0.15 for ZnO:Zn. This information was used to set the relative scaling of the left and right y axes in Figs. 1 and 3. Clearly, both the electron luminescence fraction L_-/L_+ and the excess positron luminescence $L_+ - L_-$ depend on particles' incident kinetic energy. These values and their uncertainty have been calculated for both phosphors for the entire energy range of the experiment, and plots are provided in the Supplemental Material [20]. Of particular note is the monotonic increase of the electron luminescence fraction; in the limit of high incident particle energies, the difference between positron-induced and electron-induced luminescence is expected to become negligible compared to the total amount of luminescence produced by either species, consistent with the two previous quantitative comparisons of positron and electron luminescence that we found in the literature, both done with higher-energy beams (≥ 30 keV) [8,9].

It is clear that kinetic energy is not the only means by which positrons produce luminescence; they also do so through annihilation with electrons. Annihilation produces at least one hole per positron; it can also initiate the Auger process (in which a second electron from a higher energy level falls into the hole produced by annihilation with the first, and the difference in energy between the two levels is imparted to a third electron), resulting in two holes and one excited electron [21–24] (or more, in the event of an Auger cascade [25–28]). Annihilation with core electrons is relatively unlikely; when it does occur, an excited electron

can have a kinetic energy significantly larger than the original incident positron and thereby excite additional electron-hole pairs through collisions, but this is still only in the tens or hundreds of electron-volts [22,29]. (Thus, this particular pathway is not expected to contribute significantly to the large effect we observe, in which positrons with a few electron-volts or tens of electron-volts of energy produce as much luminescence as kilo-electron-volt-scale electrons.) Annihilation with valence electrons is much more probable, and recent studies in graphene found that 80%–100% of deep valence-band holes were filled via an Auger transition [24]. When the valence band is wide enough (e.g., 20 eV in graphene), electrons excited by these "*VVV* transitions" have sufficient energy to overcome the work function, escape the material, and be observed in the positron-annihilation-induced Auger electron spectrum (PAES); in materials with narrower valence bands, *VVV* transitions may instead excite electrons merely into the conduction band, where they cannot be detected with PAES. In luminescent materials, however, conduction-band electrons can then travel to luminescence centers and there combine with valence-band holes to produce photons. Additionally, if luminescence centers involve defects that act as positron traps—e.g., certain types of vacancies [3,5,15]—positrons will preferentially annihilate there, creating holes directly at those locations in the crystal structure. Thus, there is significant potential for positron luminescence to provide new information about open questions regarding luminescent materials, which may include the structure of luminescence centers [3,4], the excitation and relaxation pathways [1,5], and/or the origin of the dead voltage [2,6].

Several mechanisms for the dead voltage have been proposed over the decades. One explanation is a nonluminescent surface layer (formed during the phosphor production process), through which electrons must penetrate in order to reach the phosphor and excite electron-hole pairs [17]. A second explanation is an enhanced propensity for nonradiative recombination of electrons and holes near the surface due to surface states and/or band bending [2]. A third explanation proposes that if a phosphor particle is coated with any insulating contaminant, however thin, a "surface bound electron layer" [Fig. 4(a)] will form, extending several micrometers into the vacuum from the surface; stabilized by a layer of subsurface holes, this creates a region of negative electrostatic potential, akin to those seen on insulators in scanning electron microscopes [30], that incident electrons must have enough energy to penetrate [1,6]. Because positrons and electrons are oppositely charged but have similar characteristics with respect to penetration into solids [12,13] and secondary electron production [31], comparing $g_+(V)$ to $g_-(V)$ can help us to discriminate among these possibilities.

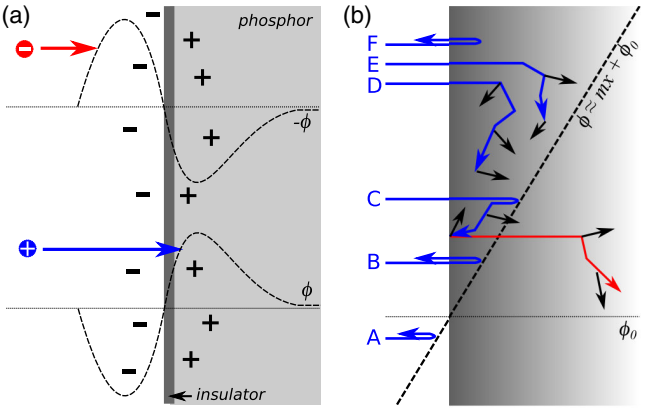

FIG. 4. (a) Illustration of a surface-bound electron layer, stabilized by a subsurface population of holes. The resulting electrostatic potential ϕ (dashed line) prevents low-energy electrons (but not positrons) from reaching the surface of the material. (b) There are many different mechanisms by which positrons interact with the phosphor surface (gray) and/or, if present, a subsurface electrostatic potential (dashed line). These include electrostatic reflection (trajectories A, B, C), inelastic collisions (C, D, E), annihilation with a core electron (C), annihilation with valence electrons (D, E), and backscattering (F). Blue arrows represent positrons, the red arrow represents an electron excited by Auger processes following core annihilation, and black arrows represent both conduction-band electrons and valence-band holes, which then lead to luminescence.

That positrons in ZnS:Ag produce significant luminescence well below the dead voltage is consistent with the third model, as the others would be expected to inhibit positron-induced luminescence in a similar fashion to electron-induced luminescence. (Note that there are not known to be Auger processes capable of producing

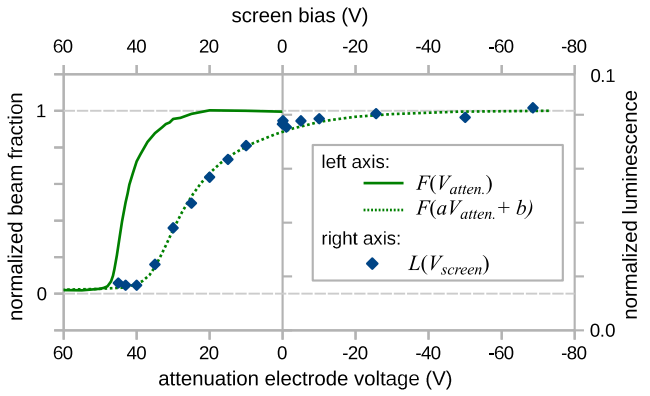

FIG. 5. The ZnS:Ag positron luminescence cutoff is plotted on the right y axis as a function of screen bias (diamond symbols); uncertainties are on the order of the symbol size. Plotted on the left y axis are the cumulative energy distribution of the beam (solid green line) and the transformation of this curve (dotted green line), as discussed in the text, that provides the best match to the cutoff ($a = 3$, $b = -103$). Horizontal dashed lines indicate normalized beam fractions of 0% and 100%.

electrons with energies above the dead voltage with nonvanishing probabilities [22].) Whereas the negative electrostatic potential of the surface bound electron layer prevents low-energy electrons from accessing the phosphor surface entirely, low-energy positrons can reach the surface and then undergo various elastic and inelastic processes [Fig. 4(b)]. Furthermore, Fig. 5 shows that the relationship between the ZnS:Ag positron luminescence cutoff and the positron beam's cumulative energy distribution $F(V_{\text{atten}})$ is consistent with the presence of a subsurface electrostatic potential ϕ that increases linearly with depth [Fig. 4(b)]. In this picture, the likelihood that positrons with just enough kinetic energy to access the surface (trajectories B and C in Fig. 4) will undergo inelastic scattering—ultimately leading to luminescence—is proportional to path length in the material. Path length (restricted by ϕ) rises linearly with incident energy. As a result, instead of occurring at the beam energy—as one would expect and as is observed for ZnO:Zn—the $L(V)$ cutoff is offset and stretched by constants relating to the potential at the surface and the length scale over which it rises.

In summary, we have performed quantitative comparisons of the luminescence produced by 0- to 5-keV positron and electron beams incident on phosphors and found that positrons produce more brightness than electrons over the entire energy range. Of particular note is that positrons with an incident energy of just a few electron-volts (in the case of ZnO:Zn) or a few tens of electron-volts (in the case of ZnS:Ag) produce as much luminescence as 2.5- to 3.5-keV electrons. These findings are expected to have significant utility for nonperturbatively diagnosing low-energy positron beams and plasmas (relevant to electron-positron pair plasma creation, antihydrogen experiments, slow positron scattering processes, and positronium ionization studies, among other applications). They also represent compelling evidence for the excitation of luminescence via annihilation and Auger processes, as well as a new way of addressing decades-old questions in cathodoluminescence.

This work has been funded by the Helmholtz Association Postdoc Programme (E. V. S.). The authors would also like to thank the Surko Group (University of California, San Diego) for the loan of their positron source; M. Otte for contributing a sample of ZnO:Zn; J. R. Danielson for the tip about producing an electron beam from the moderator; B. L. Standley, J. Horn-Stanja, and C. Richter for valuable discussions; and X. Sarasola and N. Paschkowski for their assistance in assembling the experiment.

*evs@ipp.mpg.de

[1] L. Ozawa and M. Itoh, Cathode ray tube phosphors, Chem. Rev. **103**, 3835 (2003).

[2] B. L. Abrams and P. H. Holloway, Role of the surface in luminescent processes, Chem. Rev. **104**, 5783 (2004).

[3] J. Ji, A. M. Colosimo, W. Anwand, L. A. Boatner, A. Wagner, P. S. Stepanov, T. T. Trinh, M. O. Liedke, R. Krause-Rehberg, T. E. Cowan, and F. A. Selim, ZnO Luminescence and scintillation studied via photoexcitation, X-ray excitation, and gamma-induced positron spectroscopy, Sci. Rep. **6**, 31238 (2016).

[4] P. A. Rodnyi and I. V. Khodyuk, Optical and luminescence properties of zinc oxide (Review), Opt. Spectrosc. **111**, 776 (2011).

[5] C. S. Kang, P. Beverley, P. Phipps, and R. H. Bube, Photoelectronic processes in ZnS single crystals, Phys. Rev. **156**, 998 (1967).

[6] M. Itoh and L. Ozawa, Cathodoluminescent phosphors, Annu. Rep. Prog. Chem., Sect. C: Phys. Chem. **102**, 12 (2006).

[7] J. R. Danielson, D. H. E. Dubin, R. G. Greaves, and C. M. Surko, Plasma and trap-based techniques for science with positrons, Rev. Mod. Phys. **87**, 247 (2015).

[8] K. Gubernator, P. Heckmann, and A. Flammersfeld, Die Szintillations-Lichtausbeute von Anthrazen für Positronen und Elektronen kleiner Energie, Z. Phys. **158**, 268 (1960).

[9] O. I. Meshkov, V. V. Smaluk, D. P. Sukhanov, E. N. Galashov, V. Dorokhov, A. N. Zhuravlev, and V. A. Kiselev, Experimental comparison of performance of various fluorescent screens applied for relativistic electron/positron beam imaging, in *Proceedings of the 10th European Workshop on Beam Diagnostics and Instrumentation for Particle Accelerators* (Joint Accelerator Conferences, Hamburg, Germany, 2011), p. 558.

[10] J. Xu, L. D. Hulett, Jr., T. A. Lewis, and N. H. Tolk, Studies of positron induced luminescence from polymers, Mater. Sci. Forum **175-178**, 245 (1995).

[11] S. Mukherjee, M. P. Nadesalingam, P. Guagliardo, A. D. Sergeant, B. Barbiellini, J. F. Williams, N. G. Fazleev, and A. H. Weiss, Auger-Mediated Sticking of Positrons to Surfaces: Evidence for a Single-Step Transition from a Scattering State to a Surface Image Potential Bound State, Phys. Rev. Lett. **104**, 247403 (2010).

[12] S. Valkealahti and R. M. Nieminen, Monte-Carlo calculations of keV electron and positron slowing down in solids, Appl. Phys. A **32**, 95 (1983).

[13] P. J. Schultz and K. G. Lynn, Interaction of positron beams with surfaces, thin films, and interfaces, Rev. Mod. Phys. **60**, 701 (1988).

[14] M. J. Puska and R. M. Nieminen, Theory of positrons in solids and on solid surfaces, Rev. Mod. Phys. **66**, 841 (1994).

[15] C. Hugenschmidt, Positrons in surface physics, Surf. Sci. Rep. **71**, 547 (2016).

[16] S. T. Martin and L. B. Headrick, Light output and secondary emission characteristics of luminescent materials, J. Appl. Phys. **10**, 116 (1939).

[17] J. D. Kingsley and J. S. Prener, Voltage dependence of cathode-ray efficiency of phosphors: phosphor particles with nonluminescent coatings, J. Appl. Phys. **43**, 3073 (1972).

[18] D. E. Gutzler, The efficiency of $Y_2O_2S:Tb$ under low energy electron bombardment, J. Electrochem. Soc. **126**, 571 (1979).

[19] S. Myhajlenko, Cathodoluminescence, in *Luminescence of Solids*, edited by D. R. Vij (Plenum Press, New York, 1998), ISBN 9781461553618.

[20] See Supplemental Material at http://link.aps.org/supplemental/10.1103/PhysRevLett.120.147401 for additional details of the luminescence measurements and the analysis thereof.

[21] A. Weiss, R. Mayer, M. Jibaly, C. Lei, D. Mehl, and K. G. Lynn, Auger-Electron Emission Resulting from the Annihilation of Core Electrons with Low-Energy Positrons, Phys. Rev. Lett. **61**, 2245 (1988).

[22] K. O. Jensen and A. Weiss, Theoretical study of the application of positron-induced Auger-electron spectroscopy, Phys. Rev. B **41**, 3928 (1990).

[23] E. Jung, H. Zhou, J. Kim, S. Starnes, R. Venkataraman, and A. Weiss, Background-free Auger line shape of Ag $N_{2,3}VV$ measured with positron annihilation induced Auger electron spectroscopy, Appl. Surf. Sci. **116**, 318 (1997).

[24] V. A. Chirayath, V. Callewaert, A. J. Fairchild, M. D. Chrysler, R. W. Gladen, A. D. Mcdonald, S. K. Imam, K. Shastry, A. R. Koymen, R. Saniz, B. Barbiellini, K. Rajeshwar, B. Partoens, and A. H. Weiss, Auger electron emission initiated by the creation of valence-band holes in graphene by positron annihilation, Nat. Commun. **8**, 16116 (2017).

[25] M. Wolfsberg and M. L. Perlman, Multiple electron excitation in Auger processes, Phys. Rev. **99**, 1833 (1955).

[26] L. Partanen, Ph.D. thesis, University of Oulu, 2007.

[27] V. Stumpf, K. Gokhberg, and L. S. Cederbaum, The role of metal ions in X-ray-induced photochemistry, Nat. Chem. **8**, 237 (2016).

[28] D. You, H. Fukuzawa, Y. Sakakibara, T. Takanashi, Y. Ito, G. G. Maliyar, K. Motomura, K. Nagaya, T. Nishiyama, K. Asa, Y. Sato, N. Saito, M. Oura, M. Schöffler, G. Kastirke, U. Hergenhahn, V. Stumpf, K. Gokhberg, A. I. Kuleff, L. S. Cederbaum, and K. Ueda, Charge transfer to ground-state ions produces free electrons, Nat. Commun. **8**, 14277 (2017).

[29] P. Palmberg *et al.*, *Handbook of Auger Electron Spectroscopy: A Reference Book of Standard Data for Identification and Interpretation of Auger Electron Spectroscopy Data* (Physical Electronics Industries, Edina, MN, 1972).

[30] M. Belhaj, O. Jbara, M. N. Filippov, E. I. Rau, and M. V. Andrianov, Analysis of two methods of measurement of surface potential of insulators in SEM: electron spectroscopy and X-ray spectroscopy methods, Appl. Surf. Sci. **177**, 58 (2001).

[31] E. Jung, R. Venkataraman, S. Starnes, and A. H. Weiss, The study of secondary electrons and redistributed primaries (electrons and positrons) from Ge(100) surface utilizing the electron and the positron beams, Mater. Sci. Forum, **255-257**, 708 (1997).